The structure of mixed H2O-OH monolayer films on Ru(0001)

Tatarkhanov, M.; Fomin, E.; Salmeron, M.; Andersson, Klas Jerker; Ogasawara, H.; Pettersson, L.G.M.; Nilsson, A.; Cerda, J.I.

Published in:
Journal of Chemical Physics

Link to article, DOI:
10.1063/1.2988903

Publication date:
2008

Document Version
Publisher's PDF, also known as Version of record

The structure of mixed H_2O-OH monolayer films on Ru(0001)

M. Tatarkhanov,[1,2] E. Fomin,[1,2] M. Salmeron,[1,3,a)] K. Andersson,[4,5,6] H. Ogasawara,[4] L. G. M. Pettersson,[5] A. Nilsson,[4,5] and J. I. Cerdá[7]
[1]*Lawrence Berkeley National Laboratory, Berkeley, California 94720, USA*
[2]*Physics Department, University of California, Berkeley, California 94720, USA*
[3]*Materials Science and Engineering Department, University of California, Berkeley, California 94720, USA*
[4]*Stanford Synchrotron Radiation Laboratory, Menlo Park, California 94025, USA*
[5]*FYSIKUM, Albanova University Center, Stockholm University, 106 91 Stockholm, Sweden*
[6]*Center for Individual Nanoparticle Functionality, Department of Physics, Technical University of Denmark, DK-2800 Lyngby, Denmark*
[7]*Instituto de Ciencia de Materiales de Madrid, CSIC, Cantoblanco, 28049 Madrid, Spain*

(Received 9 July 2008; accepted 4 September 2008; published online 20 October 2008)

Scanning tunneling microscopy (STM) and x-ray absorption spectroscopy (XAS) have been used to study the structures produced by water on Ru(0001) at temperatures above 140 K. It was found that while undissociated water layers are metastable below 140 K, heating above this temperature produces drastic transformations, whereby a fraction of the water molecules partially dissociate and form mixed H_2O-OH structures. X-ray photoelectron spectroscopy and XAS revealed the presence of hydroxyl groups with their O–H bond essentially parallel to the surface. STM images show that the mixed H_2O-OH structures consist of long narrow stripes aligned with the three crystallographic directions perpendicular to the close-packed atomic rows of the Ru(0001) substrate. The internal structure of the stripes is a honeycomb network of H-bonded water and hydroxyl species. We found that the metastable low temperature molecular phase can also be converted to a mixed H_2O-OH phase through excitation by the tunneling electrons when their energy is 0.5 eV or higher above the Fermi level. Structural models based on the STM images were used for density functional theory optimizations of the stripe geometry. The optimized geometry was then utilized to calculate STM images for comparison with the experiment. © *2008 American Institute of Physics*.
[DOI: 10.1063/1.2988903]

I. INTRODUCTION

The most stable structure of a layer of water on Ru(0001) has theoretically been predicted to consist of a mixture of H_2O and OH.[1,2] Experimental evidence from low energy electron diffraction (LEED) supports the mixed H_2O-OH nature of the stable layer. It also shows that the layer has a domain structure with narrow dimensions in one direction.[3–5] This is in contrast to the extended two-dimensional (2D) hydrogen (H)-bonding network formed on Pt(111)[6–12] and with similar models on Ru(0001) put forward based on theoretical modeling.[1,2] The detailed structure of the stable H_2O-OH phase on Ru(0001) remains unclear to date. Historically, some confusion was generated by the fact that the adsorption of water on Ru at low temperature, below approximately 140 K, results in films of intact molecules that are kinetically stabilized. A thermal treatment is necessary to overcome the activation barrier for the transformation of the metastable phase to the stable mixed H_2O-OH phase.[13–15]

Understanding the dissociation of water and the structure of the resulting H_2O-OH phase is important as these are involved in many industrial reactions. The facile water dissociation on Pt/Ru alloys has been invoked to explain the superior CO tolerances of these alloys compared to pure Pt in fuel cell applications during the H_2 or methanol electro-oxidation reactions.[16] In the so-called bifunctional mechanism,[17] the proposed lower activation barrier for water dissociation on Ru sites compared to Pt sites facilitates the generation of OH_{ads} which reduces the CO coverage by oxidation to CO_2.[17,18]

Compared to the large body of work accumulated on the water-Pt interface and the mixed H_2O-OH intermediate phases involved in the reaction $H_2+O_2 \rightarrow H_2O$, and water splitting reactions for H_2 production,[6–12,19–21] very little is known about the local structure and chemical properties of the mixed H_2O-OH phase on Ru. Establishing the nature of this phase has become increasingly relevant in view of reports that a low coverage of Pt islands on Ru-surfaces is more electrocatalytically active than the Pt/Ru alloy surface.[22] The properties of the mixed H_2O-OH phase on Ru(0001) could affect possible OH spillover from Ru to neighboring Pt sites.[23]

In this paper, we describe the results of a study using core-level spectroscopies, x-ray photoelectron spectroscopy (XPS), and x-ray absorption spectroscopy (XAS) to identify the species present on the surface and their orientation, and scanning tunneling microscopy (STM) to determine the structures formed by water adsorption on Ru(0001) after heating above 140 K. We found that as predicted, H_2O and OH are produced and that they form elongated stripes with an internal honeycomb structure. Geometrical models based

a)Author to whom correspondence should be addressed. Electronic mail: mbsalmeron@lbl.gov.

on STM images were used as starting points and optimized by density functional theory (DFT) calculations. These structures were then used in STM image simulations to compare with the experiments.

II. EXPERIMENTAL

The STM and the core-level spectroscopy experiments were performed on two different instruments. In both cases, clean well-ordered Ru(0001) surfaces were prepared in ultrahigh vacuum. The cleaning procedure consisted of noble gas ion bombardment, while the sample was subjected to heating and cooling cycles from 550 to 1100 K. The surface of the sample prepared in this way contained a few impurities, observed in the STM images as protrusions or depressions, present in amounts less than 0.2% of a monolayer.

The STM experiments were performed on a variable-temperature instrument capable of imaging from 40 to 300 K.[24] The instrument has been described in detail elsewhere.[25,26] The background pressure in the chamber was always below 1×10^{-10} Torr.

The XPS and polarization dependent near-edge O 1*s* XAS experiments were performed at the elliptically polarized undulator beamline 11.0.2 of the Advanced Light Source in Berkeley. The XAS and XPS spectra were recorded with a total energy resolution of about 0.1 eV. X-ray and electron damage effects[5,13,15] were negligible as a result of minimizing the photogenerated and inelastically scattered electrons down to a total of ~0.03 e^-/water.[13]

III. THEORETICAL METHODS

Total energy calculations based on DFT were performed for a variety of H_2O and OH configurations on Ru(0001). The substrate was modeled using a slab containing three Ru layers. The 2D unit cells were always rectangles of the type $(\sqrt{3}\times n)$, with n ranging from 6 to 10. Mixed H_2O-OH models in the form of stripes periodic along the $\sqrt{3}$ direction and finite in width (2 to 7 Ru lattice constants) in the perpendicular direction were constructed based on the experimental STM images. The initial geometries were then relaxed via total energy minimizations.

All the DFT calculations were performed using the SIESTA code[27] employing the generalized gradient approximation scheme[28] for the exchange and correlation parts of the energy. Troullier–Martins[29] pseudopotentials were used to replace the core electrons. A double-zeta plus polarization atomic orbital (AO) basis set was chosen for all species except for the Ru *d* states, which were described by just a single-zeta shell in order to reduce the computational cost. However, we checked in some cases that increasing the AO basis set did not alter significantly the final geometries. All atoms in the slabs were allowed to relax until the forces acting on them were smaller than 0.05 eV/Å, except for the bottom Ru layer that was fixed to the bulk positions.

We performed STM image simulations for each of the structures in order to compare with the experimental images. We employed the GREEN code[30] for these simulations, which has been extensively used for other related systems.[31–33] In these simulations, we used the relaxed slab geometry to construct a semi-infinite surface on top of which a semi-infinite W tip with a sharp single atom terminated apex is positioned at a distance of just a few angstroms. The elastic current crossing the STM interface is then calculated and the tip height adjusted so that a prefixed current value is attained. All electronic interactions are approximated with the extended Hückel theory (EHT), with the associated parameters (on-site energies and Slater orbitals) obtained after fitting the EHT electronic structure to that derived from the *ab initio* DFT calculations.[34]

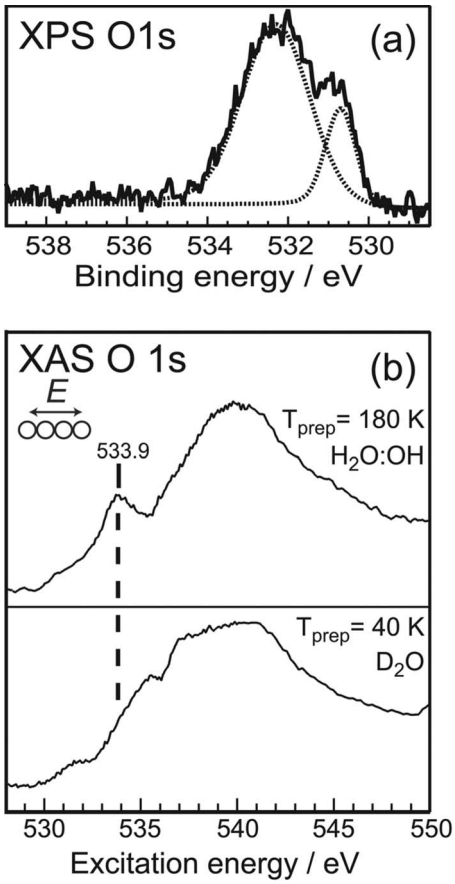

FIG. 1. O 1*s* core-level spectra of the H_2O-OH phase and molecularly intact water clusters on Ru(0001). (a) O 1*s* XPS ($h\upsilon$=785 eV) acquired at 90 K after adsorption of ~2 L of H_2O at 180 K. The two peaks correspond to OH at 530.8 eV and molecular H_2O at 532.3 eV. (b) Top: O 1*s* x-ray absorption spectrum of the H_2O-OH phase in (a), recorded at 90 K. The x rays are polarized with the *E*-field parallel to the surface. The intense peak observed at 533.9 eV is assigned to the $4\sigma^*$ resonance of flat-lying nondonor O–H bonds. Bottom: Similar spectrum for ~0.17 ML molecularly intact water clusters, (D_2O), prepared and acquired at 40 K. The in-plane resonance near 535 eV is related to uncoordinated D in D_2O.

IV. RESULTS

A. XPS and XAS results

Figure 1(a) shows the O 1*s* XPS region of a surface prepared by dosing ~2 L H_2O at 180 K. We observe an O 1*s* peak at 530.8 eV due to OH and a 532.3 eV peak due to molecular H_2O,[13,15,35] which provides evidence that the phase formed by annealing H_2O at 180 K contains both H_2O and OH. Calibrating against the ~0.67 ML saturation coverage of the metastable intact water monolayer obtained by

desorbing water multilayers from a sample at 150 K,[13,15] the total O coverage in the mixed phase deduced from the O 1*s* peak area is 0.22 ± 0.02 ML, of which OH constitutes $23 \pm 3\%$. This leads to a OH coverage of ~0.05 ML. A slightly different preparation procedure where ~4 MLs molecular H_2O, adsorbed at 90 K, are annealed to 180 K (heating rate ~0.5 K s^{-1}) resulted in a similar H_2O:OH ratio and total coverage. These results are consistent with other work that found that OH constitutes only $30\% \pm 10\%$ of the coverage of the mixed H_2O–OH structure on Ru(0001) formed either thermally or by electron bombardment, and also by coadsorption of H_2O (D_2O) with small amounts of atomic O.[13–15,35]

The XAS at the O 1*s* edge gives information on the O 2*p* unoccupied electronic states. Using the polarization dependence of the absorption process, we obtain information on bond orientation. The spectra obtained with the *E*-vector parallel to the Ru(0001) surface probe the 2D in-plane H-bonding network with sensitivity to the local coordination of the H atoms. Significant differences are observed in the spectra of the film formed at low temperature and after annealing. As shown in Fig. 1(b), a distinct in-plane resonance at 533.9 eV is observed in the in-plane XAS spectrum from the H_2O–OH layer, which is absent in intact water layers formed at lower temperature, as shown in the figure (obtained for D_2O).

Taking into account a $2(\pm 0.5)$ eV difference between the energy scales of our XAS spectra and that of Ref. 36, the in-plane XAS low energy resonance from the H_2O–OH phase is also present, and even more prominent, in a surface prepared by heating at a slightly higher temperature (185 K). The feature is also observed as a shoulder in Ref. 37 for a H_2O–OH layer prepared at lower temperature (165 K); its weak relative intensity is explained by a likely higher H_2O/OH ratio at this lower temperature. The results suggest possible preparation dependent H_2O–OH structures, and hence the varying intensity of the ~534 eV in-plane XAS peak. The nature of the 533.9 eV in-plane XAS resonance has not been addressed previously, but is thoroughly discussed in Sec. V B.

B. STM results: thermal treatment

STM images acquired before and after heating above 175 K revealed profound changes in the structure and coverage of the water film. Figure 2(a) shows a STM image of the film of water formed by dosing water at 40 K followed by annealing at 130 K. The hexagonal network of the flat ice layer is clearly visible. Experimental and theoretical studies have established that the structure of this low temperature phase consists of a molecular network of H-bonded molecules alternating between nearly flat and vertical molecules on top of Ru sites.[5,13] Figures 2(b) and 2(c) show the result of annealing to 180 K a 3–4 ML film of H_2O initially adsorbed at 45 K. The heating reduced the coverage to less than 1 ML and drastically changed the structure of the layer. In contrast to the extended hexagonal structures of Fig. 2(a), elongated islands or stripes aligned perpendicular to the close-packed atomic rows of the Ru(0001) substrate are now

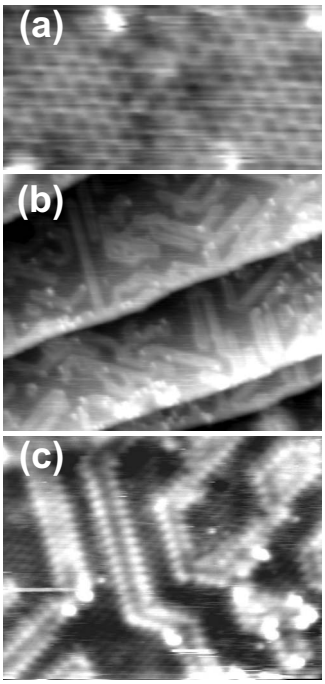

FIG. 2. STM topography images of water on Ru(0001) obtained before (a) and after [(b) and (c)] heating to 180 K that produces partial dissociation of water. (a) STM image (~50×25 Å^2), acquired at 40 K using scanning parameters +120 mV/280 pA. Extended honeycomb structures were formed after heating to 130K. (b) STM image (~700×600 Å^2), obtained after dosing 3–4 ML H_2O at 40 K followed by annealing to 180 K. Scanning parameters were +100 mV and 230 pA. Elongated structures are formed which are perpendicular to the close-packed atomic directions. (c) Close-up STM image (~150×120 Å^2), acquired at 40 K using scanning parameters +0.67 mV/870 pA. Elongated islands (stripes) decorated by bright edges are clearly visible. In this image the region between the water stripes is covered by H forming a $\sqrt{3} \times \sqrt{3}$ phase. The H is a result of water dissociation and also adsorption from the background gas.

present. Figure 2(c) shows a high resolution STM image of the stripes. The edges of the narrow stripes are decorated by high contrast features (bright spots). Between stripes a $\sqrt{3} \times \sqrt{3}$ periodic structure of low contrast features (dark spots) is formed. This structure is recognized as the $(\sqrt{3} \times \sqrt{3})$-1*H* phase created by atomic hydrogen, product of partial dissociation of water in the water phase, with some additional amount of hydrogen possibly adsorbed from residual gas phase H_2 in the system. The same $\sqrt{3} \times \sqrt{3}$ structure was observed after molecular hydrogen dissociative adsorption on clean Ru.[38,39] Another view of the stripes and their internal structure is shown in Fig. 3. A honeycomb structure can be observed inside the stripes. The most salient characteristic of the stripes is their narrow width, between one and three hexagonal cells (2.5 and 6 Ru lattice distances respectively), and the bright protrusions decorating their perimeters. Although not visible in this image, H is also present on the surface as a result of water decomposition. It is visible as $(\sqrt{3} \times \sqrt{3})$ periodicity formed by dark spots in between bright stripes in Fig. 2(c). Prolonged exposure to water at 180 K produced a higher coverage of stripes, with widths of 3.5, 4, and 5 Ru lattice constants lying parallel to each other in three directions perpendicular to the substrate lattice. Analysis of these stripes reveals a weak periodicity of the stripes with correlation distances between 6 and 8 Ru lattice constants.

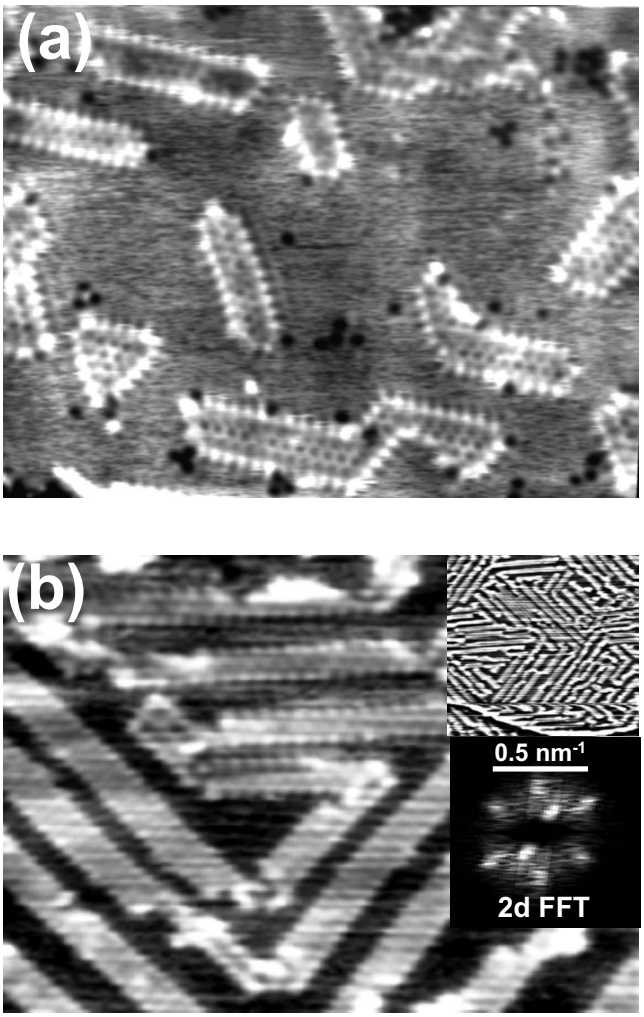

FIG. 3. (a) STM image ($\sim 200\times 160$ Å^2 size) of the structure formed by dosing 3–4 ML H_2O at 45 K and subsequent annealing to 180 K. Image was acquired at 45 K with scanning parameters +90 mV/180 pA. The internal structure of the mixed H_2O-OH phase can be resolved and consists of elongated honeycomb structures with high contrast periphery. The dark spots are due to impurity atoms (C and O). H atoms are also present but cannot be resolved in this image due to their weak contrast and rapid mobility. (b) STM image ($\sim 200\times 130$ Å^2 size) of the structure formed by dosing more than 5 ML of H_2O at 45 K and subsequent annealing to 180 K. Image was acquired at 45 K with scanning parameters +80 mV/215 pA. Stripes aligned into three directions perpendicular to Ru lattice directions are clearly visible. Correlation of distances between adjacent stripes was measured to be from 6 to 8 Ru lattice constants. A weak honeycomb internal structure is visible in some of the stripes. Upper inset image shows larger (400×400 Å^2) area showing a pseudoperiodic superstructure of the stripes. The lower inset image is the corresponding 2D-FFT pattern. Six hexagonal spots in the pattern correspond to three directions of pseudoperiodic superstructure of the stripes. The underlying hexagonal Ru(0001) substrate is not visible; therefore, it does not form a diffraction pattern in this image.

This superstructure can give rise to the splitting of the main spots in the LEED pattern observed in Refs. 3–5. Indeed, 2D-fast Fourier transform (FFT) analysis of STM image in Fig. 3(b) shows this splitting (lower inset). The six hexagonal spots in the 2D-FFT pattern correspond to three alignment directions of the pseudoperiodic superstructure of the stripes.

C. STM results: tip induced dissociation

Some of the initial confusion in the literature as to whether the thermodynamically stable water monolayer are made of pure intact molecules or contains partially dissociated molecules is related to the fact that in many experiments using probe particles or radiation, electrons in LEED and secondary electrons and x rays in XPS, the dissociation of water is highly enhanced.[5,13,15] To assess this beam-induced dissociation, we investigated the effect of tunneling electrons from the tip at various bias voltages and currents. We found that electrons can convert the low temperature molecular H_2O layer into a film with structure similar to that produced by heating. This is shown in the images of Fig. 4. The top image shows three terraces separated by monatomic steps of the Ru(0001) surface. The surface was initially covered by a poorly ordered multilayer film of water deposited at 35 K (two to three layers). The roughly square depression in the middle terrace was caused by scanning that area with a bias voltage of 0.6 V and 10 nA of tunneling current. This produced a strong modification in the water film structure. Most of the water layers above the first were displaced or desorbed by the tip. In addition the remaining first layer is modified and shows a structure of elongated stripes very similar to that produced by thermal annealing. This is shown in the magnified images (b) and (c) of Fig. 4, acquired at the center of the square in (a). These electron induced changes were observed to occur only when the bias was above 0.5 V.

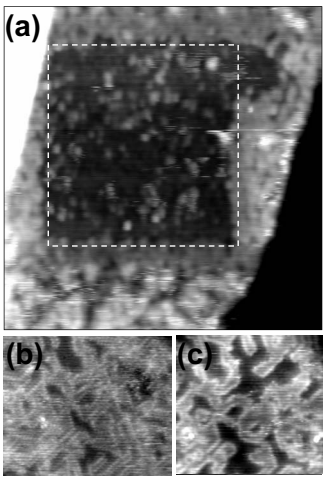

FIG. 4. Tip induced changes in water layer on Ru(0001). (a) STM image (400×400 Å^2) acquired at 40 K for 2 ML water coverage on Ru(0001). The 200×200 Å^2 dark square at the center of the image shows the effect of the tip on the water structure when scanning was performed with increased parameters +0.6 V (sample)/10 nA. [(b) and (c)] Close-up images of regions inside the modified square region showing elongated stripes with bright edge decoration similar to Figs. 2(b) and 2(c).

V. DISCUSSION

We start the discussion by analyzing first the structure of the mixed H_2O-OH stripes observed by STM, with the help of theoretical calculations. A representative collection of striped structures extracted from several STM images is shown in Fig. 5(a) (left column). Their structure is made of hexagonal cells in a honeycomb arrangement. They form narrow stripes varying in width from one to three or four hexagonal cells, corresponding to 2.5–6 Ru lattice constants. A distinctive characteristic of the images is the appearance of

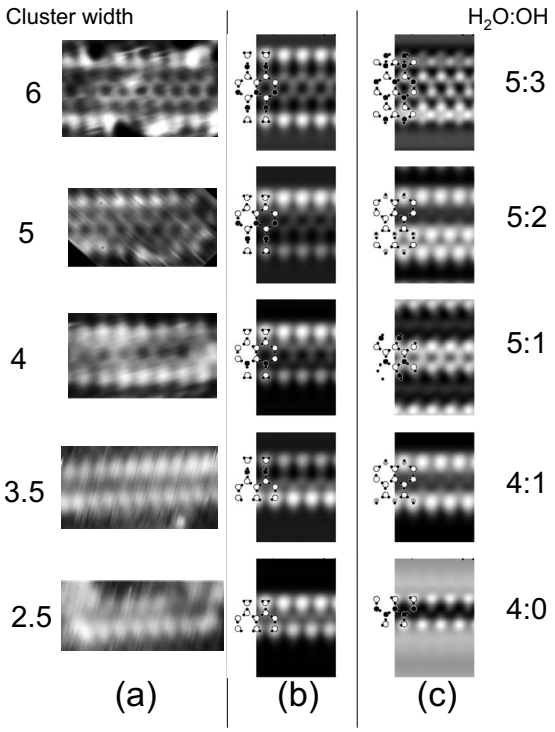

FIG. 5. (a) Close-up images showing various types of mixed H_2O-OH honeycomb stripes extracted from larger scale STM images. The numbers to the left give the width of the stripe in the image in units of Ru–Ru atomic distances. (b) STM simulations for the models that best fit each cluster. Drawings of the H_2O and OH species forming the stripe are superimposed in the left part of the calculated images with white and dark circles, respectively. The H atoms appear as small dark circles in all cases. The bright edges are due to nondonor water molecules. The models were obtained by DFT optimization of initial structures where H_2O or OH was placed at the nodes of the hexagons suggested by the STM images. After relaxation OH appeared always inside the cluster, even when initially placed at the edges. (c) Alternative models and their associated STM images following the same scheme as in (b). Nonflat water molecules (tilted or down) are depicted by gray circles.

bright features decorating the edges. The location of these features is such that they are aligned with the center of the hexagon in the central part.

A. STM simulations

Close to 40 different models were explored theoretically using initial geometries based on the STM images. In the models we placed a water molecule or a OH group at each node of the honeycomb structure suggested by the experimental image. For the edges of the stripes, we considered a variety of H_2O and OH geometries, including close-packed arrangements where the OH species were adsorbed at top, bridge, and threefold sites, and tilted water molecules. We found a different metastable energy minimum for almost all models considered, which implies that the total energy landscape is very complex, with many local minima. Energetic arguments alone cannot discriminate between the different phases since kinetics may well restrict the accessibility of the system to the most stable states. A few relevant energetic trends could be extracted from the calculations:

(i) The H_2O molecules prefer to lay flat rather than tilted and all molecules bond to the substrate exclusively via the oxygen atoms. This is in accordance with previous findings summarized in the so-called 2D water rules[32,33] and also with results for the extended H-bonded mixed H_2O/OH phases on Pt(111).[6–12] The oxygen atoms in the H_2O and OH molecules are nearly coplanar, with a small corrugation of approximately 0.2 Å, which can reach a value of 0.5 Å at the edges. In a separate study of the water structures formed on Pd and Ru at temperatures below 140 K, we observed that individual water molecules are often attached to the edges of single hexamers or clusters containing several hexagons. These attached molecules have a high contrast (producing bright spots in a gray scale image).[32]

(ii) The H_2O (donor)–OH (acceptor) bonding is more stable than the H_2O-H_2O bonding by about 100 meV, although variations in the presence and precise location of the atomic H adsorption site within the stripe may reduce this difference to just a few tens of meV.

(iii) There is a strong preference for the OH groups to be inside the stripes rather than at the edges. For example, for some structures we found that after relaxation OH groups initially placed with a dangling H at the edges "migrated" to the interior of the cluster via proton transfer from adjacent molecules.

After obtaining simulated STM images for each of the models and comparing them with the experimental data, we found that the structures that best fit the observed images are those displayed in Fig. 5(b) (central column). We note that the OH species are always located inside the cluster and that the simulated images compare reasonably well with the experimental ones for all widths. In contrast, simulations for stripes where OH groups were forced to sit at the edges consistently failed to reproduce the experimentally observed enhanced signal along the perimeter of the stripes. In all cases, the optimized geometry has both H_2O and OH groups on top of Ru sites, binding through the O lone pair to the metal. The H-bond network is fully saturated inside the clusters, with no dangling H bonds and all O–H bonds between water and hydroxyl essentially parallel to the surface, in agreement with the XAS results, as discussed below. The binding to the substrate is stronger for OH groups than for water molecules, hence the former tend to be closer to the substrate; the oxygen adsorption height is between 2.1 and 2.2 Å for the hydroxyls and between 2.2 and 2.4 Å for the water molecules within the cluster. The OH species inside the stripe (only present for the widest models 5 and 6) tend to reduce the buckling among adjacent oxygen atoms, thus favoring a planar geometry. While O–O distances between water molecules (2.6–2.8 Å) are close to the Ru lattice constant, the O–O distance between water (as donor) and hydroxyls (as acceptor) tends to be smaller (2.4–2.6 Å).

Another important result of the calculations is that in all models, the edge species always consists of a single H-bond acceptor H_2O molecule with the two dangling H pointing away from the cluster. These edge water molecules are attached to the peripheral water molecule or OH group with the O–H bond oriented perpendicular to the edge. In the

former case (model 2.5, bottom edge in 3.5 and top edges in 4 and 5), they are always the most buckled species in the stripe, with O adsorption heights of 2.7–2.9 Å and both dangling H tilted toward the surface by 0.5 Å below the O.[32] In the STM simulations they always provide an enhanced contrast with respect to the internal molecules in the stripe, in agreement with the bright features at the edges. When the edge molecule is attached to a OH (upper edge in model 3.5 and lower edges in 5 and 6), the H bond is weaker with an O–O distance of up to 3.0 Å, so that the edge molecule can adopt a more planar geometry resembling the isolated molecule case. The oxygen adsorption height decreases to 2.4–2.5 Å, but it is still larger than that within the network (2.2–2.4 Å) leading again to a bright maxima albeit slightly less intense. The presence of such OH groups linked to the edge molecules explains why in some clusters the location of the maxima is displaced by one lattice spacing from the nodes of the $(\sqrt{3}\times\sqrt{3})$ lattice, although this is difficult to infer from the experimental images of Fig. 5(a). It is also consistent with the fact that the enhanced brightness experimentally observed at the cluster edges varies among clusters or between the upper and lower edges within the same stripe.

The H_2O to OH ratios for each model stripe are indicated on the right side of the figure. They vary from 4:0 to 5:3. This range of values fits reasonably well with the 3:1 ratio determined experimentally from XPS as an average of different cluster values. Finally, the calculated corrugation of the stripes, ranging between 0.6 and 0.9 Å, is in good agreement with the experimental value of around 0.7 Å.

The right column of Fig. 5(c) shows STM simulations corresponding to less stable alternative structures for each stripe width. We include these cases in order to show the sensitivity of the simulated images to different models. A flat single-donor H_2O with just one dangling H does not provide enough contrast enhancement at the edges (models 2.5 or 4). On the other hand, OH placed at the edges (models 6 and 4) yield a smaller contrast and cannot account for the bright edge features. Tilted edge water molecules whereby the edge species accepts two H bonds and has the dangling H pointing away from the cluster, one above the O and the other one below (models 3.5 and 5), provide too large contrast, with an apparent height larger than 0.9 Å. Further, they are energetically less stable than single acceptor flat H_2O.[32] Too large apparent heights are also obtained if nonflat H_2O are included within the clusters (see model 5 where a water molecule with a H pointing toward the substrate has been inserted).

B. XPS and XAS

Unsaturated H bonds (uncoordinated H) give rise to distinct O 1*s* XAS low energy resonances ($h\nu \leq 537$ eV) [40–44] that can explain the 533.9 eV in-plane XAS resonance observed for the H_2O–OH stripes. These unsaturated H bonds are significantly flat lying (parallel to the surface) based on the observed polarization dependent XAS spectra, in agreement with the STM results, as well as with electron energy loss spectroscopy (EELS) studies[48] and IR data[14] of the mixed H_2O–OH phase.

Nondonor H_2O (i.e., both H uncoordinated) gives rise to sharp resonances at 534 and 536 eV for water in the gas phase.[40,41] A stripe termination with nondonor H_2O at the perimeter as predicted by the STM results is consistent with the ~534 eV resonance in XAS. Interestingly, we note in Fig. 1(b) that a sharp 536 eV resonance, expected to be about twice as intense as the 534 eV resonance,[40,41] is not observed. This may be due to the bonding to the Ru(0001) surface in combination with the nondonor H_2O accepting a H bond, giving rise to some modifications in intensity ratio and resonance energy,[41] respectively. However, with the absence of the expected sharp and intense 536 eV resonance, we should also consider configurations other than the nondonor H_2O that could be responsible for the 533.9 eV feature, although they appear less likely alternatives based on the STM modeling.

Single-donor H_2O (i.e., donating one H bond and the other H unsaturated) normally gives rise to a resonance at 535 eV,[40–42] and this can explain the 535 eV feature for water at the edges of the intact water clusters.[45] However, when there are other H in the vicinity of the uncoordinated H, the 535 eV resonance can shift down to the 533–534 eV range.[43] It cannot be excluded that such a particular situation can arise due to the water dissociation leaving H_{ads} in a threefold hollow site below the uncoordinated H of a single-donor H_2O at the perimeter of the H_2O–OH stripe.

The third possibility is that the 533.9 eV resonance stems from uncoordinated H in OH (hydroxyl). In solution a 532.9 ± 0.3 eV XAS resonance related to hydroxyl has recently been observed.[44] The hydroxyl H is uncoordinated based on neutron diffraction determining the average OH (donor)-H_2O (acceptor) O–O distance to ~3.5 Å,[46] whereas the H_2O (donor)-OH (acceptor) O–O distance is as short as ~2.3 Å. We note that it may not be necessary for OH to be located at the perimeter of the stripes. From the structural DFT optimizations for H_2O–OH/Ru(0001), we observe very similar structural H_2O–OH donor-acceptor H-bond length asymmetries as for H_2O–OH on Pt(111).[12] With some further asymmetry for particular local configurations inside the H_2O–OH stripes on Ru(0001), the H in OH could become essentially uncoordinated and produce the 533.9 eV resonance.

C. Comparison to previously suggested structures of the H_2O–OH phase

Concerning the qualitative features and larger-scale structure of the H_2O–OH phase, it is clear that the observed finite-sized stripe structures differ drastically from the extended H-bonding network models put forward previously based on theoretical modeling.[1,2,47] However, the stripe structures rationalize previous LEED results obtained above 150 K,[3–5] with the most commonly observed stripe widths (four to six Ru lattice parameters) comparing favorably with widths of 4.5 to 6.5 lattice parameters estimated in Ref. 4. Furthermore, the essentially flat-lying nature of H_2O and OH in the stripes observed in our combined STM and XAS study is fully consistent with previous IR data[14] and agrees with the theoretical predictions.[1,2,47]

A novel and well-defined OH-stretch peak at 3565 cm^{-1} induced by H_2O adsorption at $165 < T \leq 200$ K is observable in EELS (Ref. 48) but not in IR.[14] Contrary to extended H-bond saturated models, the observed finite-sized H_2O-OH stripes with flat-lying nondonor species (uncoordinated H) at the perimeter can account for the 3565 cm^{-1} nondonor OH stretch.

Where quantitative results exist, e.g., experimental[49] and theoretical[1,2,47] Ru–O distances, our DFT results suggest Ru–OH distances of 2.1–2.2 Å and $Ru-OH_2$ distances of 2.2–2.4 Å inside the various stripe models. This compares well with the experimental values of 2.08 ± 0.02 Å and 2.23 ± 0.02 Å. Whereas previous theoretical studies underestimate the $Ru-OH_2$ distance by ~0.07 Å compared to experiment, our results tend to slightly overestimate this value.

D. Electron induced dissociation

The results described in Sec. IV C demonstrate very clearly the high susceptibility of the O–H bonds to electronically induced excitations. In particular, the threshold value of 0.5 V of the bias voltage to induce the transformation from intact to partially dissociated water structures is close to the energy of the O–H stretch mode of the molecule, which is also the reaction coordinate for dissociation, as has been shown recently in our laboratory.[50] Another interesting observation that emanates from our experiments is that once partially dissociated into H_2O+OH clusters, the water structure is more stable and does not dissociate further unless high energy electrons are utilized.

VI. CONCLUSIONS

A stable partially dissociated H_2O-OH phase of water adsorbed on Ru(0001) was produced by heating to 180 K. XPS and XAS revealed that both H_2O and OH are present with an average ratio of 3:1. The O–H bonding configuration is such that the bonds are mostly parallel to the surface. STM imaging revealed that the mixed H_2O-OH phase has a honeycomb structure forming elongated stripes with widths most commonly observed in the range of four to six Ru(0001) lattice parameters.

Theoretical DFT calculations in combination with STM image simulations allowed us to test a large number of different models for the observed striped structures, which helped interpret the experimental observations. Models where nondonor single acceptor H_2O molecules are located at periphery positions and OH groups in the interior of the stripes were found to be most stable by DFT calculations, and their simulated STM images provided a good match with the experimental images.

The 3:1 ratio of H_2O to OH measured by XPS also matches very well with the average ratios from the models that best match the experimental images.

Finally, we have shown that the low temperature molecular water layer can be converted to the mixed H_2O-OH phase via excitation by the tunneling electrons in the STM, in analogy to conversion of low temperature water phase to partially dissociated phase. For such electron induced conversion, the tunneling electron energy must be larger than 0.5 eV, which points to the excitation of O–H stretch mode as the main reason for the dissociation.

ACKNOWLEDGMENTS

This work was supported by the Director, Office of Science, Office of Basic Energy Sciences, and Materials Sciences and Engineering Division of the U. S. Department of Energy under Contract No. DE-AC02-05CH11231. The theoretical work was supported by the Spanish Ministry of Science and Technology (Project No. MAT2007-66719-C03-02). The XPS and XAS work was supported by the NSF (Grant No. CHE-0089215) grant and by the Swedish Foundation for Strategic Research, Swedish Natural Science Research Council. The staff, David Shuh, Mary Gilles, and Tolek Tyliszczak at beamline 11.0.2, Advanced Light Source, are gratefully acknowledged.

[1] P. J. Feibelman, Science **295**, 99 (2002); Chem. Phys. Lett. **410**, 120 (2005).
[2] A. Michaelides, A. Alavi, and D. A. King, J. Am. Chem. Soc. **125**, 2746 (2003).
[3] D. L. Doering and T. E. Madey, Surf. Sci. **123**, 305 (1982).
[4] G. Held and D. Menzel, Surf. Sci. **327**, 301 (1995).
[5] S. Haq, C. Clay, G. R. Darling, G. Zimbitas, and A. Hodgson, Phys. Rev. B **73**, 115414 (2006).
[6] S. Völkening, K. Bedürftig, K. Jacobi, J. Wintterlin, and G. Ertl, Phys. Rev. Lett. **83**, 2672 (1999); K. Bedürftig, S. Völkening, Y. Wang, J. Wintterlin, K. Jacobi, and G. Ertl, J. Chem. Phys. **111**, 11147 (1999).
[7] A. P. Seitsonen, Y. Zhu, K. Bedürftig, and H. Over, J. Am. Chem. Soc. **123**, 7347 (2001).
[8] A. Michaelides and P. Hu, J. Chem. Phys. **114**, 513 (2001); J. Am. Chem. Soc. **123**, 4235 (2001).
[9] G. S. Karlberg and G. Wahnström, Phys. Rev. Lett. **92**, 136103 (2004).
[10] G. Held, C. Clay, S. D. Barrett, S. Haq, and A. Hodgson, J. Chem. Phys. **123**, 064711 (2005).
[11] C. Clay, S. Haq, and A. Hodgson, Phys. Rev. Lett. **92**, 046102 (2004).
[12] T. Schiros, L.-Å. Näslund, K. Andersson, J. Gyllenpalm, G. S. Karlberg, M. Odelius, H. Ogasawara, L. G. M. Pettersson, and A. Nilsson, J. Phys. Chem. C **111**, 15003 (2007).
[13] K. Andersson, A. Nikitin, L. G. M. Pettersson, A. Nilsson, and H. Ogasawara, Phys. Rev. Lett. **93**, 196101 (2004).
[14] C. Clay, S. Haq, and A. Hodgson, Chem. Phys. Lett. **388**, 89 (2004).
[15] N. S. Faradzhev, K. L. Kostov, P. Feulner, T. E. Madey, and D. Menzel, Chem. Phys. Lett. **415**, 165 (2005).
[16] H. F. Oetjen, V. M. Schmidt, U. Stimming, and F. Trila, J. Electrochem. Soc. **143**, 3838 (1996).
[17] M. Watanabe and S. Motoo, J. Electroanal. Chem. **60**, 267 (1975); **60**, 275 (1975).
[18] J. C. Davies, B. E. Hayden, and D. J. Pegg, Surf. Sci. **467**, 118 (2000); P. Liu, A. Logadottir, and J. K. Nørskov, Electrochim. Acta **48**, 3731 (2003).
[19] P. A. Thiel and T. E. Madey, Surf. Sci. Rep. **7**, 211 (1987).
[20] M. A. Henderson, Surf. Sci. Rep. **46**, 1 (2002).
[21] H. Ogasawara, B. Brena, D. Nordlund, M. Nyberg, A. Pelmenschikov, L. G. M.Pettersson, and A. Nilson, Phys. Rev. Lett. **89**, 276102 (2002).
[22] R. R. Adzic, J. Zhang, K. Sasaki, M. B. Vukmirovic, M. Shao, J. X. Wang, A. U. Nilekar, M. Mavrikakis, J. A. Valerio, and F. Uribe, Top. Catal. **46**, 249 (2007), and references therein.
[23] J. C. Davies, B. E. Hayden, D. J. Pegg, and M. E. Rendall, Surf. Sci. **496**, 110 (2002).
[24] The cryogenic system was described in (Ref. 25), The STM head used here was similar to that in (Ref. 26), where the tip and scanner were enclosed in a copper thermal shield and were at the same temperature.
[25] S. Behler, M. K. Rose, J. C. Dunphy, D. F. Ogletree, and M. Salmeron, Rev. Sci. Instrum. **68**, 2479 (1997).
[26] F. Mugele, Ch. Kloos, P. Leiderer, and R. Moller, Rev. Sci. Instrum. **67**, 2557 (1996).
[27] J. M. Soler, E. Artacho, J. Gale, A. García, J. Junquera, P. Ordejón, and

D. Sánchez-Portal, J. Phys.: Condens. Matter **14**, 2745 (2002).
[28] J. P. Perdew, Phys. Rev. B **46**, 6671 (1992).
[29] N. Troullier and J. L. Martins, Phys. Rev. B **43**, 1993 (1991).
[30] J. Cerdá, M. A. Van Hove, P. Sautet, and M. Salmeron, Phys. Rev. B **56**, 15885 (1997); see http://www.icmm.csic.es/jcerda/ for further details.
[31] T. K. Shimizu, A. Mugarza, J. Cerda, M. Heyde, Y. Qi, U. D. Schwarz, D. F. Ogletree, and M. Salmeron, J. Phys. Chem. C **112**, 7445 (2008).
[32] M. Tatarkhanov, F. Rose, E. Fomin, T. Mitsui, M. Rose, J. Cerdá, and M. Salmeron, "Growth and structure of water monolayers on Pd(111) and Ru(0001) surfaces studied by STM at low temperature (<130 K)," Surf. Sci. (in press).
[33] J. Cerdá, A. Michaelides, M.-L. Bocquet, P. J. Feibelman, T. Mitsui, M. Rose, E. Fomin, and M. Salmeron, Phys. Rev. Lett. **93**, 116101 (2004).
[34] J. Cerdá and F. Soria, Phys. Rev. B **61**, 7965 (2000).
[35] J. Weissenrieder, A. Mikkelsen, J. N. Andersen, P. J. Feibelman, and G. Held, Phys. Rev. Lett. **93**, 196102 (2004).
[36] D. Coulman, A. Puschmann, U. Höfer, H.-P. Steinrück, W. Wurth, P. Feulner, and D. Menzel, J. Chem. Phys. **93**, 58 (1990).
[37] M. J. Gladys, A. A. El-Zein, A. Mikkelsen, J. N. Andersen, and G. Held, Phys. Rev. B **78**, 035409 (2008).
[38] M. Tatarkhanov, F. Rose, E. Fomin, D. F. Ogletree, and M. Salmeron, Surf. Sci. **602**, 487 (2008).
[39] F. Rose, M. Tatarkhanov, E. Fomin, and M. Salmeron, J. Phys. Chem. **111**, 050 (2007).
[40] S. Myneni, Y. Luo, L. A. Näslund, L. Ojamae, H. Ogasawara, A. Pelmenschikov, P. Wernet, P. Väterlein, C. Heske, Z. Hussein, L. G. M. Pettersson, and A. Nilsson, J. Phys.: Condens. Matter **14**, L213 (2002).
[41] M. Cavalleri, H. Ogasawara, L. G. M. Pettersson, and A. Nilsson, Chem. Phys. Lett. **364**, 363 (2002).
[42] P. Wernet, D. Nordlund, U. Bergmann, M. Cavalleri, M. Odelius, H. Ogasawara, L.-Å. Näslund, T. K. Hirsch, L. Ojamäe, P. Glatzel, L. G. M. Pettersson, and A. Nilsson, Science **304**, 995 (2004); D. Nordlund, H. Ogasawara, P. Wernet, M. Nyberg, M. Odelius, L. G. M. Pettersson, and A. Nilsson, Chem. Phys. Lett. **395**, 161 (2004).
[43] M. Leetmaa, M. Ljungberg, H. Ogasawara, M. Odelius, L.-Å. Näslund, A. Nilsson, and L. G. M. Pettersson, J. Chem. Phys. **125**, 244510 (2006); T. Schiros, H. Ogasawara, K. Andersson, J. MacNaughton, H. Öström, O. Takahashi, L.G. M. Pettersson, and A. Nilsson (unpublished).
[44] O. Fuchs, M. Zharnikov, L. Weinhardt, M. Blum, M. Weigand, Y. Zubavichus, M. Bär, F. Maier, J. D. Denlinger, C. Heske, M. Grunze, and E. Umbach, Phys. Rev. Lett. **100**, 027801 (2008); C. D. Cappa, J. D. Smith, B. M. Messer, R. C. Cohen, and R. J. Saykally, J. Phys. Chem. A **111**, 4776 (2007).
[45] K. Andersson, H. Ogasawara, M. Odelius, L. G. M. Pettersson, and A. Nilsson (unpublished).
[46] A. Botti, F. Bruni, S. Imberti, M. A. Ricci, and A. K. J. Soper, Chem. Phys. **120**, 10154 (2004).
[47] G. Materzanini, G. F. Tantardini, P. J. D. Lindan, and P. Saalfrank, Phys. Rev. B **71**, 155414 (2005).
[48] P. A. Thiel, R. A. DePaola, and F. M. Hoffman, J. Chem. Phys. **80**, 5326 (1984).
[49] G. Held and D. Menzel, Surf. Sci. **316**, 92 (1994).
[50] A. Mugarza, T. K. Shimizu, D. F. Ogletree, J. Cerda, and M. Salmeron (unpublished).